

NUP98–HOXA9 expression in hemopoietic stem cells induces chronic and acute myeloid leukemias in mice

Evert Kroon¹, Unnur Thorsteinsdottir¹, Nadine Mayotte¹, Takuro Nakamura² and Guy Sauvageau^{1,3,4,5}

¹Laboratory of Molecular Genetics of Hemopoietic Stem Cells, Clinical Research Institute of Montréal, Montréal, Québec, H2W 1R7, ³Département de Médecine, Université de Montréal, Montréal, Québec, H3J 3J7, ⁴Département d'Hématologie, Hôpital Maisonneuve-Rosemont, Montréal, Québec, H1T 2M2 Canada and ²Department of Carcinogenesis, The Cancer Institute, Tokyo, Japan

⁵Corresponding author
e-mail: sauvagg@ircm.qc.ca

Here we describe hemopoietic chimeras serving as a mouse model for NUP98–HOXA9-induced leukemia, which reproduced several of the phenotypes observed in human disease. Mice transplanted with bone marrow cells expressing NUP98–HOXA9 through retroviral transduction acquire a myeloproliferative disease (MPD) and eventually succumb to acute myeloid leukemia (AML). The NUP98 portion of the fusion protein was shown to be responsible for transforming a clinically silent pre-leukemic phase observed for Hoxa9 into a chronic, stem cell-derived MPD. The co-expression of NUP98–HOXA9 and Meis1 accelerated the transformation of MPD to AML, identifying a genetic interaction previously observed for Hoxa9 and Meis1. Our findings demonstrate the presence of overlapping yet distinct molecular mechanisms for MPD versus AML, illustrating the complexity of leukemic transformation.

Keywords: AML/Hox/Meis/NUP98–HOXA9/PBX

Introduction

The nucleoporin NUP98 gene on chromosome 11p15 is involved in relatively rare but recurring translocations observed in *de novo* acute and chronic leukemias, as well as therapy-related myelodysplastic syndrome (t-MDS) and acute myeloid leukemia (t-AML) (Borrow *et al.*, 1996; Nakamura *et al.*, 1996a, 1999; Arai *et al.*, 1997; Raza-Egilmez *et al.*, 1998; Ikeda *et al.*, 1999; Nishiyama *et al.*, 1999). Among the target genes in these translocations are several homeobox genes, including PMX1 (on chromosome 1q23) (Nakamura *et al.*, 1999) and HOXD13 (2q31) (Raza-Egilmez *et al.*, 1998), while unidentified targets on 12q13 and 17q21 may involve genes of the HOXB and HOXC clusters, respectively (Nishiyama *et al.*, 1999). The most frequent target of 11p15 translocations is homeobox gene HOXA9 (7p15) and while t(7;11)(p15;p15) is predominantly observed in patients with AML (Borrow *et al.*, 1996; Nakamura *et al.*, 1996a), cases of chronic diseases have been reported as well (Inaba *et al.*, 1996; Hatano *et al.*, 1999; Wong *et al.*,

1999). The importance of HOXA9 in human leukemias was also demonstrated in an analysis of 6817 genes in leukemias of poor prognosis, which found the most highly correlating factor to be the expression of HOXA9 (Golub *et al.*, 1999).

The leukemogenic potential of murine Hoxa9 was directly assessed in hemopoietic chimeras where its over-expression in bone marrow cells induced AML after a latency period (Kroon *et al.*, 1998). In addition, Meis1 together with Hoxa7 or -a9 is a frequent target of endogenous retroviral insertional activation in the leukemic cells of the BXH-2 mice (Nakamura *et al.*, 1996b), suggesting a leukemogenic collaboration between Meis1 and Hox genes. In support of this, the co-expression of Meis1 dramatically reduced the latency of AML induced by Hoxa9 (Kroon *et al.*, 1998) and Hoxb3 (Thorsteinsdottir *et al.*, 2001). Meis1 and other members of the Meis subfamily of homeoproteins have been shown to interact with and direct the nuclear localization of PBX homeoproteins (Chang *et al.*, 1997; Rieckhof *et al.*, 1997; Berthelsen *et al.*, 1999). The results from *in vitro* fibroblast transformation assays suggest that HOX proteins, including Hoxa9, require the presence of and interaction with PBX proteins (Krosl *et al.*, 1998; Kasper *et al.*, 1999; Schnabel *et al.*, 2000), with which they form heterodimeric DNA-binding complexes (Chang *et al.*, 1995; Phelan *et al.*, 1995). A trimeric DNA-binding complex composed of Hoxa9, Pbx2 and Meis1 has been detected in leukemic cell lines and it has been suggested that leukemogenesis by Hoxa9 may require the formation of such a complex (Shen *et al.*, 1999; Schnabel *et al.*, 2000). However, *in vitro* immortalization of myeloid progenitor cells by Hoxa9 was reported to occur in the absence of Meis expression and Hoxa9–PBX interaction (Calvo *et al.*, 2000), suggesting that HOX-induced transformation might also occur independently of collaborators in the Meis and PBX families. PBX-independent functions in hemopoietic cells have also been described *in vitro* and *in vivo* for HOXB4 (Beslu *et al.*, 2000).

In all chimeric NUP98–homeoprotein fusions described to date, the N-terminal portion of NUP98 is fused to the C-terminal portion of its partner, which includes the DNA-binding homeodomain (Borrow *et al.*, 1996; Nakamura *et al.*, 1996a, 1999; Raza-Egilmez *et al.*, 1998). NUP98 was shown to confer potent transcriptional activity onto its partner in NUP98–PMX1 (Nakamura *et al.*, 1999) and NUP98–HOXA9, and in the latter this appears to be mediated through CBP/p300 (Kasper *et al.*, 1999). NUP98–HOXA9 has also been shown to form a cooperative DNA-binding complex with PBX1, and its capacity to transform NIH 3T3 cells appears to require this interaction (Kasper *et al.*, 1999). These data suggest that leukemogenesis through NUP98–HOXA9 may require

nuclear PBX, implicating a potential role for *Meis1* as well.

We evaluated the leukemogenic potential of *NUP98–HOXA9* through retroviral transduction and transplantation of bone marrow cells. The results indicated that *NUP98–HOXA9* and *Hoxa9* share the capacity to induce AML and collaborate with *Meis1*, but that *NUP98–HOXA9* is unique in its potential to induce a pre-leukemic MPD.

Results

***NUP98–HOXA9* transplantation chimeras develop a chronic MPD**

To determine whether the expression of *NUP98–HOXA9* could transform hemopoietic cells, the fusion protein was expressed in primary bone marrow cells through retroviral gene transfer. Figure 1A–C shows schematic representations of the fusion protein and the MSCV retrovirus, and demonstrates that the latter directs the expression of the appropriate protein in infected cells. Directly following retroviral infection of bone marrow cells, *NUP98–HOXA9* had no detectable effects on the *in vitro* differentiation and hemopoietic growth factor requirement of myeloid colony forming cells (CFC) in semi-solid cultures (data not shown). However, the abnormally large size of the colonies that grew in such cultures suggested that *NUP98–HOXA9*-transduced bone marrow progenitors acquired a marked increase in their proliferative potential (data not shown). Consistent with this, *NUP98–HOXA9*-expressing cells replated more efficiently (Figure 1D, >60 randomly selected colonies analyzed per group) and the colonies generated in the secondary cultures were much larger than the controls (Figure 1E). Interestingly, the replating efficiency of *Hoxa9*- and *NUP98–HOXA9*-transduced cells was similar (87 and 88%, respectively), but fewer and smaller secondary *Hoxa9* colonies were observed (data not shown). Thus, while *NUP98–HOXA9* expression does not appear to affect *in vitro* differentiation of primary bone marrow cells, it induces a dramatic increase in their proliferative capacity.

To assess whether the expression of *NUP98–HOXA9* in bone marrow cells could induce leukemia in mice, several transplantation experiments were performed. Table I shows the dose of transduced cells that were transplanted per mouse in three independent experiments. At 2 months post-bone marrow transplantation (BMT), *NUP98–HOXA9* chimeras had moderately increased numbers of peripheral white blood cells (13 ± 10 versus 3.6 ± 0.7 in control mice, average \pm standard deviation $\times 10^9/l$, $n = 4$ for both groups), mainly due to neutrophils and monocytes (Figure 2A; and data not shown). There was a marked increase in the size of platelets observed in the peripheral blood of these mice (Figure 2A). To characterize this chronic condition and its evolution, *NUP98–HOXA9* mice were sacrificed at 2 and 8 months post-BMT. *NUP98–HOXA9* mice sacrificed early (2 months) post-BMT had no overt hemopoietic anomalies, but showed a 2- to 3-fold increase in the numbers of myeloid CFC in the bone marrow and spleen (Table II). In mice analyzed at 8 months post-BMT, the spleen was increased 3-fold in size and contained 30-fold more myeloid CFC than control mice (Table II). The majority of

the CFC gave rise to colonies containing granulocytes and/or macrophages (CFU-GM; $n = 50$ colonies analyzed by cytological studies, data not shown). The bone marrow and spleen of *NUP98–HOXA9* mice had fewer erythroblasts (red cell precursors) and lymphocytes (Figure 2A). Myeloid infiltration was not detected in the liver, thymus or lymph nodes of these animals as determined by cytological and FACS analyses (Figure 2A; and data not shown). In summary, *NUP98–HOXA9* expression in bone marrow cells induced an MPD in mice, characterized by increased peripheral monocyte and neutrophil numbers, platelet size and spleen CFU-GM, and progressing with time. This differs markedly from the pre-leukemic phenotype observed in *Hoxa9* hemopoietic chimeras in which no increased production of mature myeloid cells was observed (Kroon *et al.*, 1998).

***NUP98–HOXA9*-transduced cells contribute to repopulation of all lineages, but B-lymphopoiesis is impaired**

The contribution of *NUP98–HOXA9*-transduced cells (EGFP⁺) to myeloid, B- and T-cell differentiation *in vivo* was evaluated by FACS analyses (Figure 2B). In accordance with the cytological studies shown in Figure 2A, there was a marked increase in the proportion (and absolute numbers) of myeloid (Gr-1⁺ or Mac-1⁺) cells in the peripheral blood and spleen of *NUP98–HOXA9* chimeras (Figure 2B). The majority of these Gr-1⁺ or Mac-1⁺ cells were transduced (i.e. EGFP⁺), confirming the contribution of the *NUP98–HOXA9*-infected cells to myeloid repopulation and splenic infiltration. This increase in myeloid cells in *NUP98–HOXA9* mice is consistent with the marked increase observed in myeloid CFC numbers in the spleen (Table II), and in the *in vitro* proliferation/self-renewal of *NUP98–HOXA9* myeloid progenitors (Figure 1D and E).

NUP98–HOXA9-infected cells were also present in the T-lymphoid compartment (CD4⁺, CD8⁺) in the thymus, although they were under-represented as compared with *EGFP* control mice that received a lower dose of infected cells in the BMT inoculum (Figure 2B; Table I). The numbers of *NUP98–HOXA9*-infected cells were exceptionally low in the B-lymphoid (B220⁺) compartment in the peripheral blood, bone marrow and spleen (Figure 2B). Consistent with this, transduced (Neo⁺ or EGFP⁺) bone marrow pre-B lymphoid progenitors were practically undetectable in *NUP98–HOXA9* mice ($n = 5$ mice, data not shown), indicating that *NUP98–HOXA9* expression is not compatible with B-lymphopoiesis. Thus, while the production of cells of the myeloid lineage is greatly enhanced, primitive cells expressing *NUP98–HOXA9* can contribute to T-cell but not (or very inefficiently) to B-cell lineages.

The *NUP98–HOXA9*-induced MPD is a polyclonal stem cell disease

Southern blot analyses performed on genomic DNA isolated from *NUP98–HOXA9* mice indicated the presence of the intact provirus in the hemopoietic tissues but the absence of a signal in non-hemopoietic organs (Figure 2C, top panel). Confirming the results of cytological and FACS studies, *NUP98–HOXA9*-transduced cells did not invade non-hemopoietic organs of mice with MPD.

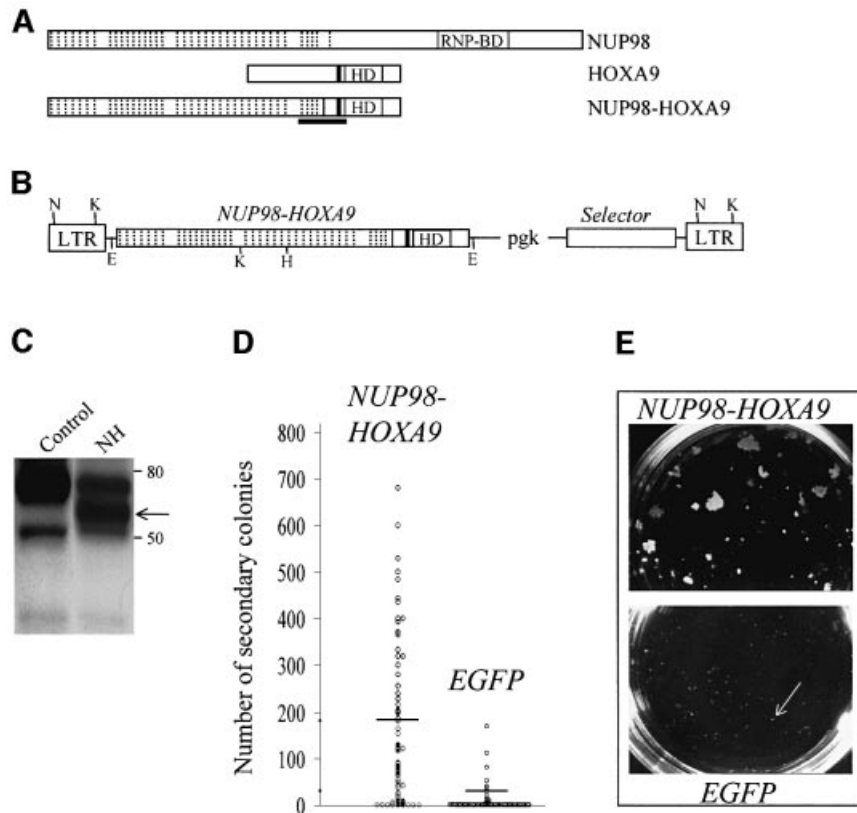


Fig. 1. Recombinant retrovirus-mediated expression of NUP98-HOXA9 in primary bone marrow cells results in enhanced proliferation *in vitro*. Schematic representations of NUP98, HOXA9 and the NUP98-HOXA9 fusion protein (A) and the MSCV (Hawley *et al.*, 1994) retroviral vector employed in these studies (B), the demonstration that the recombinant retrovirus directs the expression of the appropriate protein in infected cells (C), and that NUP98-HOXA9 expression in bone marrow cells enhances the proliferative potential of myeloid progenitor cells *in vitro* (D, E). (A) Hashed lines denote the 38 FG repeats of NUP98, 37 of which are retained in the fusion protein NUP98-HOXA9; HD, DNA-binding homeodomain; the tryptophan required for NUP98-HOXA9 and HOXA9 interaction with DNA binding partner PBX (Kasper *et al.*, 1999; Schnabel *et al.*, 2000) is represented by the black line N-terminal to the HD; the region of NUP98-HOXA9 corresponding to a peptide used to raise antibodies against the fusion protein is underlined. (B) The MSCV retroviral vector utilized in these studies directs the expression of the gene of interest from the viral LTR, while the selector gene [conferring antibiotic resistance to G418 (*Neo*) or puromycin (*Pac*), or inducing green (*EGFP*) or yellow (*EYFP*) fluorescence] is expressed from the internal pgk promoter. Restriction sites are shown for *EcoRI* (E), *HindIII* (H), *KpnI* (K) and *NheI* (N). (C) Western blot analysis of total cell extracts of NUP98-HOXA9-infected (lane NH) or control Rat-1 fibroblasts, probed with antiserum raised against a NUP98-HOXA9 peptide (see A). The positions of the 59 kDa NUP98-HOXA9 protein (arrow) and of size markers are indicated. For (D) and (E), randomly selected, individual colonies derived from freshly infected (EGFP⁺, as determined by fluorescence microscopy) bone marrow cells grown in semi-solid methylcellulose cultures were isolated, dispersed and replated in secondary cultures. (D) The number of secondary colonies that arose from each replated primary colony is shown for cells infected with the NUP98-HOXA9 and the control EGFP retroviruses. The replating efficiency, the percentage of primary colonies generating secondary colonies, was 88% for NUP98-HOXA9 (69 of 78 primary colonies analyzed, yielding an average of 181 secondary colonies per dish) and 30% for EGFP (20 of 66 colonies analyzed, yielding an average of 32 secondary colonies). Horizontal lines indicate the average number of secondary colonies. These numbers were generated from two independent bone marrow infection experiments. (E) The size of secondary colonies generated by cells expressing NUP98-HOXA9 is much larger than those derived from the control EGFP-expressing cells (indicated by arrow), as can be seen in these macroscopic views of the 3.5 cm methylcellulose culture dishes. Typical examples are shown.

Clonal analyses showed that during the course of the MPD, multiple different clones contributed to the population of NUP98-HOXA9-infected cells (Figure 2C, bottom panel). Such clones are distinguished by different autoradiographic bands visible at different intensities or in different hemopoietic organs (Figure 2C, bone marrow versus spleen of mouse #3). This poly-clonality becomes apparent for mice (e.g. #12 and #13) that were transplanted with a high BMT cell dose (Table I; Figure 2C). In mice transplanted with as few as 1–4 infected long-term repopulating cells (LTRC, see Table I), a similar number of clones (between 2 and 5) were detected (Figure 2C). The MPD phenotype was observed in mice as late as 251 or 473 days post-transplantation (time of analysis shown in Figure 2C, bottom), when of all the transduced cells transplanted only the LTRC were expected to remain.

Most importantly, clones that contributed to the myeloproliferation in the spleen were also detected in the thymus (Figure 2C, compare mouse #3, S versus T), while in none of these mice were myeloid cells detected in the thymus by cytological or FACS analyses (Figure 2B; and data not shown). This suggested that the pool of totipotent LTRC (i.e. stem cells) expressing NUP98-HOXA9 contributed to the MPD phenotype.

To investigate this further, bone marrow cells from NUP98-HOXA9 mice were transplanted into secondary recipients (10⁶ bone marrow cells into lethally irradiated mice). Clonal analyses of secondary recipients revealed that clones which contributed to the myeloproliferative disease (some of which are totipotent, e.g. Figure 2C, mouse #3 clones 'a' and 'b') in the primary mice repopulated the secondary recipients. These secondary

Table I. Dose of *NUP98–HOXA9*-transduced cells transplanted per mouse

Virus [number of mice]	ID #, symbol ^a	No. of CFC ^b transplanted per mouse		No. of infected LTRC ^c transplanted per mouse
		Total	Transduced ^d	
<i>NUP98–HOXA9</i> (<i>Neo</i>) [4]	1–4, cross	1800	144	1
<i>NUP98–HOXA9</i> (<i>EGFP</i>) [7]	5–11, cross	1750	350	4
<i>NUP98–HOXA9</i> (<i>EGFP</i>) [5]	12–16, circle	31 100	19 300	193
<i>NUP98–HOXA9</i> (<i>EGFP</i>) [2]	17, 18, diamond	11 400	6640	66
<i>EGFP-1</i> ^e [4]	–	1150	259	3
<i>EGFP-2</i> [3]	–	54 000	36 600	366
<i>EGFP-3</i> [5]	–	22 900	8470	85

^aSymbols are used to represent mice from each group in Figure 4C.

^bMyeloid colony forming cells, as measured in clonogenic progenitor assays.

^cEstimated: reported to be ~1% of transduced CFC frequency (Sauvageau *et al.*, 1995; Thorsteinsdottir *et al.*, 1999).

^dAs determined by resistance to G-418 (*Neo* viruses), or detection of fluorescence (*EGFP* viruses) either by FACS or microscopy.

^eThe group of *EGFP* mice that most resembled *NUP98–HOXA9* mice with respect to transplanted dose of transduced CFC was used when needed as controls.

Table II. Progression of MPD in *NUP98–HOXA9* hemopoietic chimeras

	Femur		Spleen		
	NC ^a × 10 ⁷	CFC ^b × 10 ³	Size (g)	NC ^a × 10 ⁷	CFC ^b × 10 ³
<i>NUP98–HOXA9</i>					
Early post-BMT ^c (<i>n</i> = 3)	1.6 ± 0.3	110 ± 18	0.15 ± 0.06	10 ± 1	19 ± 8
Late post-BMT ^d (<i>n</i> = 2)	2.3 ± 0.4	64 ± 26	0.38 ± 0.08	30 ± 5	150 ± 10
Secondary BMT ^e (<i>n</i> = 2)	4.3 ± 0.4	770 ± 170	0.37 ± 0.20	68 ± 42	1100 ± 53
<i>EGFP</i> control ^f (<i>n</i> = 3)	2.1 ± 0.1	60 ± 24	0.10 ± 0.01	13 ± 3	5.1 ± 1

^aNucleated cells.

^bMyeloid colony forming cells, as measured in progenitor assays.

^cTwo months post-BMT.

^dEight months post-BMT.

^eTransplanted with 10⁶ BM cells from early post-BMT group, sacrificed at 5 months.

^fOne mouse early, and two mice late post-BMT, pooled because identical.

mice also developed MPD (Table II), as indicated by increases in spleen size (3- to 4-fold) and cellularity (2- to 10-fold), CFC numbers (up to 200-fold), and peripheral granulocyte and monocyte counts (not shown). Examples of clonal transmission of the MPD are shown in Figure 2C (see secondary mice B.1 and B.2 of mouse #3, and B.1 of mouse #5). Clonal analysis of the secondary recipients also revealed the presence of clones undetectable in the bone marrow of primary mice. For example, clone 'c', which was predominant in the spleen of mouse #3, repopulated the bone marrow of secondary recipient B.2 (Figure 2C). In secondary mice, multiple clones contributed to the myeloid progenitors detected *in vitro* and at least some of those clones participated in lymphoid and myeloid reconstitution as determined by clonality studies (Figure 2D) and FACS (Figure 2E).

MPD was not observed in mice when myeloid progenitors from freshly infected bone marrow cells (i.e. individual colonies) were expanded *in vitro* prior to transplantation (2–10 × 10⁶ cells transplanted per mouse, 0/6 mice reconstituted, data not shown), or when bone marrow cells from *NUP98–HOXA9* mice with MPD were transplanted into non-irradiated mice (1–4 × 10⁶ cells transplanted per mouse, 1/6 mice reconstituted, data not shown). This indicated that progenitor cells expressing *NUP98–HOXA9* were not immortalized *per se*, and that conditions unfavorable to the maintenance of or marrow

reconstitution by stem cells prevented the transplantation of the MPD.

These data indicated that *NUP98–HOXA9* induced a chronic MPD, as is observed in some patients (Inaba *et al.*, 1996; Hatano *et al.*, 1999; Wong *et al.*, 1999), and strongly suggested that this disease originated from long-term lympho-myeloid repopulating (i.e. hemopoietic stem) cells.

***NUP98–HOXA9*-induced MPD progresses into AML**

After a latency of at least 4 months, 11 of 14 *NUP98–HOXA9* mice succumbed to AML (Figure 3A). The leukemic mice presented with splenomegaly (0.60 ± 0.30 g) and lymphadenopathy (5 mm), and showed infiltration by immature myeloid cells in all organs tested, including peripheral blood, bone marrow, spleen, liver (see Figure 3B), thymus, lungs and kidneys (not shown). FACS analysis indicated that the leukemic cells were predominantly myeloid (Mac-1⁺, data not shown). Two of five leukemic samples tested did not require hemopoietic growth factors for *in vitro* maintenance.

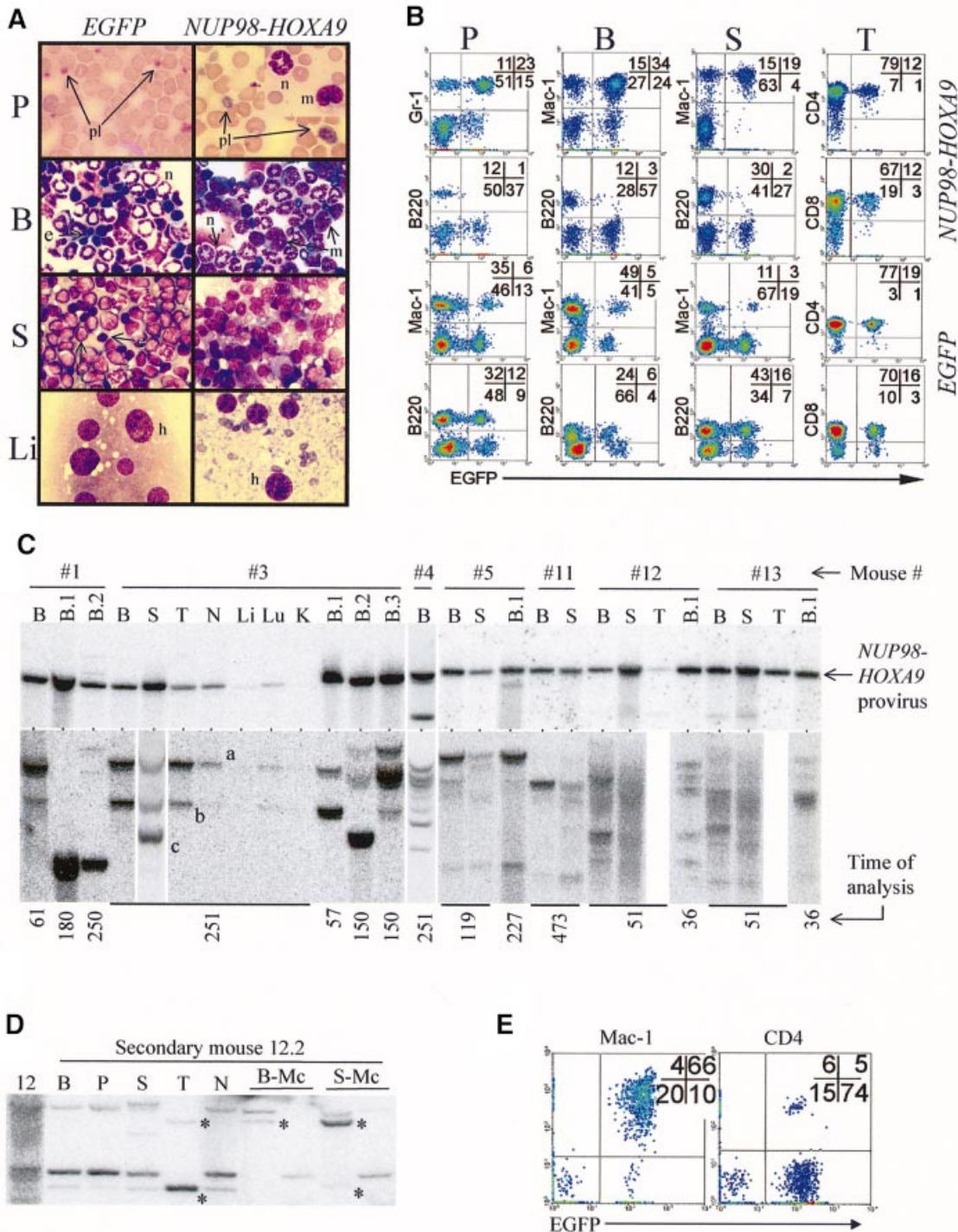
Strong Southern hybridization signals of the *NUP98–HOXA9* provirus were detected for each leukemic animal in all organs analyzed, including organs where no signal was detected in mice suffering from the *NUP98–HOXA9* MPD (e.g. the liver and kidneys, compare

Figures 2C and 3C). This confirmed that the evolution of MPD to AML is also characterized by infiltration of non-hemopoietic organs.

Clonal analysis of the leukemias showed that in contrast to the oligo-poly-clonality of the MPD, the *NUP98-HOXA9*-induced AML is predominantly mono- or bi-clonal (Figure 3C, bottom panel). While multiple clones persist in the bone marrow or spleen of some animals (Figure 3C, mouse #8), generally the predominant clone has infiltrated other organs (Figure 3C) and is transplanted to secondary recipients (see below). The presence of

multiple clones in some of these animals may account for the persistence of some characteristics of the MPD phenotype in these mice, such as large platelets (Figure 3B).

To confirm that these mice had acute leukemia, bone marrow cells from the primary mice were transplanted to non-irradiated secondary recipients. These secondary mice all succumbed to AML in 1–2 months post-transplantation, much faster than the primary animals (see shaded area in Figure 3A). Transplanting as few as 400 bone marrow cells from primary mice could rapidly reconstitute



the monoclonal AML in secondary mice, as is shown for mouse #2 in Figure 3C. Consequently, the frequency of the leukemia-repopulating cell (LRC), the cell that can reconstitute the leukemic phenotype when transplanted, exceeded 1 in 400 bone marrow cells. The difference in the latency of the disease between primary and secondary transplants indicated that the expression of *NUP98–HOXA9* in bone marrow cells alone was not sufficient to induce leukemic transformation and that an additional (genetic) event(s) was required.

The co-expression of *NUP98–HOXA9* and *Meis1a* accelerated the onset of AML

Hoxa9 expression in murine bone marrow cells has previously been shown to induce AML with a latency of several months and, while *Meis1* expression alone does not lead to AML, the co-expression of *Hoxa9* and *Meis1* is sufficient to acutely transform bone marrow cells (Kroon *et al.*, 1998). To assess whether overexpression of *Meis1* could also substitute as a transforming event in *NUP98–HOXA9* leukemogenesis, multiple hemopoietic chimeras were generated with bone marrow cells exposed to both *NUP98–HOXA9*- and *Meis1*-bearing retroviruses. Table III shows the dose of transduced bone marrow cells that were transplanted per mouse in three independent experiments.

Two months post-transplantation, three *Meis1/NUP98–HOXA9* mice were sacrificed and shown to have acquired MPD similar to the *NUP98–HOXA9* mice described above (data not shown). The contribution to the MPD of cells infected with *NUP98–HOXA9* versus both *NUP98–HOXA9* and *Meis1* was similar to that present in the initial BMT inoculum shown in Table III, as determined by FACS (Figure 4A) and myeloid progenitor assays (data not shown). Thus, the overexpression of *Meis1* did not appear to alter the MPD induced by *NUP98–HOXA9*.

After a latency of several months, *Meis1/NUP98–HOXA9* chimeras succumbed to AML of a similar phenotype as observed in the *NUP98–HOXA9* mice (Figure 4B; and data not shown). The AML in *Meis1/NUP98–HOXA9* mice was also readily transplanted to secondary recipients (9/9 tested) and as few as 100 leukemic bone marrow cells were sufficient to rapidly reproduce AML in secondary recipients. The time required for AML to develop in secondary recipients was between

26 and 58 days post-transplantation, depending on the transplanted cell dose (ranging from 1×10^6 to 100, respectively). These data and the time at which each primary mouse acquired AML are summarized in Figure 4C. Also shown is the time of AML onset in *Hoxa9* and *Meis1/Hoxa9* chimeras, which were created as control groups for these experiments. As previously reported (Kroon *et al.*, 1998), all *Hoxa9* mice survived well after all *Meis1/Hoxa9* mice had died of AML (Figure 4C). Although less dramatic, a significant difference ($p < 0.004$) is also seen between the onset of AML in *NUP98–HOXA9* mice (230 ± 67 days post-BMT) and *Meis1/NUP98–HOXA9* mice (142 ± 52 days). In contrast to *Meis1/Hoxa9*-induced AML in primary and secondary recipients, most of the primary AML in *Meis1/NUP98–HOXA9* mice required longer to develop than the secondary AML (Figure 4C). Thus, while co-expression of *Meis1* can significantly shorten the latency of *NUP98–HOXA9*-induced AML, it is not sufficient to acutely transform bone marrow cells.

Results from Southern blot analyses performed on bone marrow cells isolated from leukemic *Meis1/NUP98–HOXA9* mice provided further evidence for a genetic interaction between *Meis1* and *NUP98–HOXA9*. In the cells of 13 of 16 leukemic mice, both proviruses were present, while in the remaining three only *NUP98–HOXA9* was detected (Figure 4D). In the original BMT inoculum, only 4–25% of the *NUP98–HOXA9*-transduced cells also contained the *Meis1* provirus (Table III), whereas the majority of leukemic clones contained both proviruses (Figure 4D). In secondary recipients of bone marrow cells from these (double positive) mice, both proviruses were also detected (total of 26 secondary mice analyzed, Figure 4D; and data not shown), indicating that *Meis1/NUP98–HOXA9*-infected cells were indeed responsible for the AML.

Together these data showed that while *Meis1* did not appear to alter the myeloproliferative effect of *NUP98–HOXA9*, the progression from MPD to AML was accelerated. In contrast to *Hoxa9*, however, bone marrow cells co-expressing *NUP98–HOXA9* and *Meis1* were not acutely transformed, as the development of AML in primary mice lagged behind that in secondary mice. Thus, the expression of *Meis1* alone does not lead to the acute transformation of *NUP98–HOXA9*-expressing cells. This suggested that the N-terminal portion of *HOXA9* is required for rapid leukemogenic collaboration with *Meis1*.

Fig. 2. Characterization of *NUP98–HOXA9*-induced myeloproliferation in mice. (A) Wright-stained bloodsmear ($125\times$) and cytospin ($100\times$) preparations from representative *NUP98–HOXA9* and *EGFP* control mice. Peripheral blood, P; bone marrow, B; spleen, S; liver, Li; platelets, pl; neutrophils, n; monocytes, m; lymphocytes, l; erythroblasts, e. (B) FACS analyses of hemopoietic organs (peripheral blood, P; bone marrow, B; spleen, S; and thymus, T) of representative *NUP98–HOXA9* (#12, see Table I) and *EGFP* (*EGFP*-3 group, Table I) control mice, staining for Mac-1, Gr-1, B220, CD4 and CD8. Infected cells are identified by EGFP fluorescence. (C) In *NUP98–HOXA9* mice, the provirus is intact (top panel) and the population of *NUP98–HOXA9*-infected cells is oligoclonal (bottom panel). Top panel: Southern blot analysis assessing the integrity of the provirus shows that the 5.1 kb *NUP98–HOXA9*-bearing provirus is present and intact in the bone marrow (B) of all mice analyzed, and is also detected in the spleen (S), thymus (T), lymph nodes (N) and lung (Lu), but only weakly so in the liver (Li) and not at all in the kidneys (K). With the exception of one mouse (#4, lower band), no significant amount of rearranged provirus is detected. Bottom panel: Southern blot analysis surveying the integration sites of the proviruses. The time at which the mice were analyzed (in days post-transplantation) is shown at the bottom. For mice 1–4, membranes were hybridized to the *Neo* probe, and for all other mice the *EGFP* probe was used. Clones that contribute to myeloid colonies in secondary transplants are totipotent (D and E). (D) Clonal analysis by Southern hybridization of DNA from primary mouse #12 and a secondary recipient (12.2). B, bone marrow; P, peripheral blood; S, spleen; T, thymus; N, lymph nodes; B-Mc and S-Mc, DNA from cells harvested from bone marrow and splenic myeloid colonies grown in methylcellulose cultures, respectively. Asterisks identify totipotent clones by virtue of contribution to myeloid colonies and to reconstitution of the thymus. (E) FACS analysis confirms the contribution of *NUP98–HOXA9*-expressing (*EGFP*⁺) cells to myeloid (Mac-1) and lymphoid (CD4) lineages in the spleen of mouse #12.2. For mouse numbers refer to Table I.

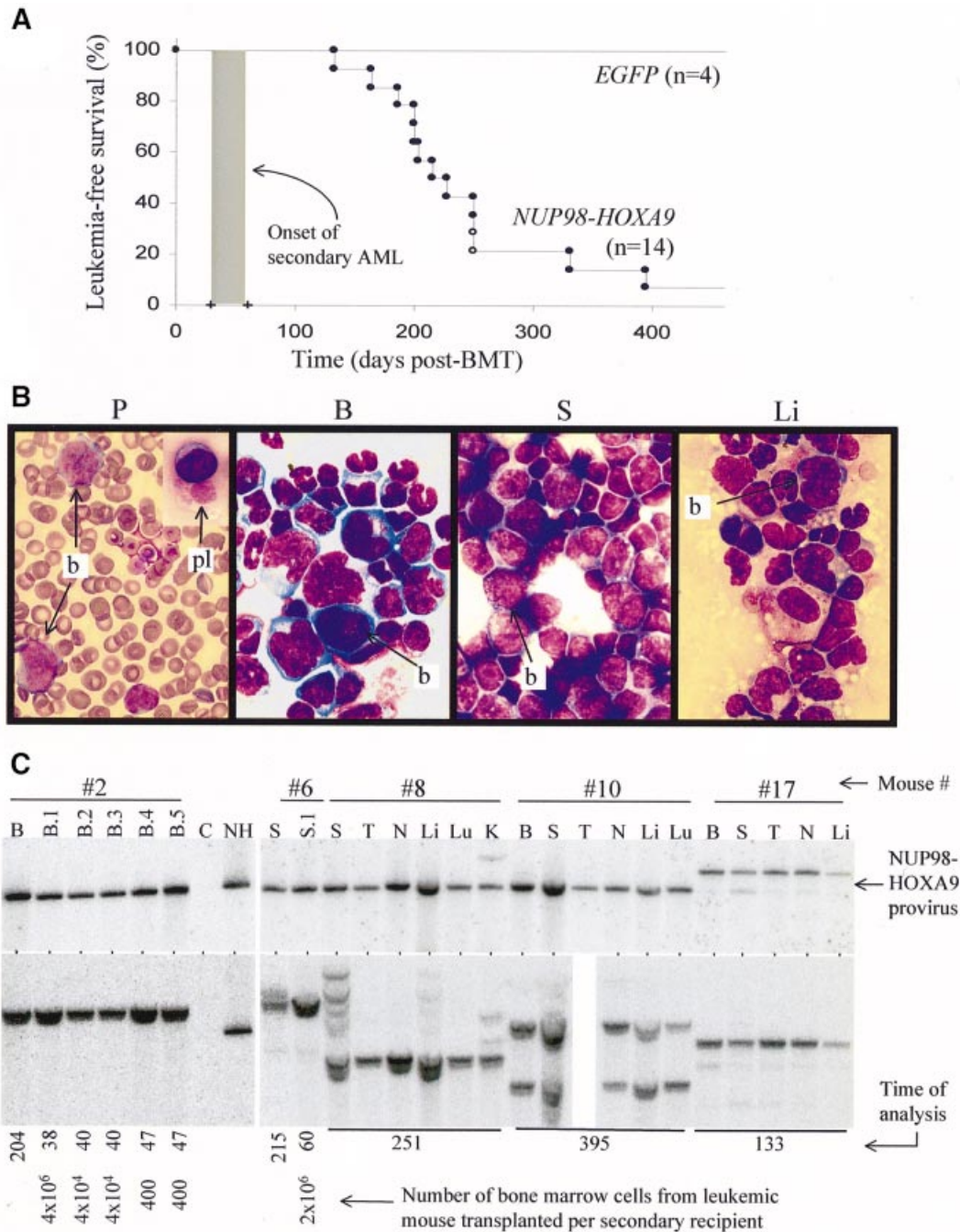


Fig. 3. *NUP98-HOXA9* induces AML in mice. **(A)** Survival curve of *NUP98-HOXA9* mice. Of the mice that were not sacrificed early ($n = 14$), 11 succumbed to AML (closed circles). The remaining three, two of which were sacrificed at 251 days post-BMT (open circles), were shown to have acquired MPD. The shaded box indicates the time at which mice succumb to secondary AML, which ranged from 25 to 60 days depending on the dose of leukemic bone marrow cells transplanted per secondary recipient. **(B)** Wright-stained cytopsin preparations (and blood smear) from a representative mouse with *NUP98-HOXA9*-induced AML show massive infiltration by immature myeloid cells (blasts, b) of the peripheral blood (P), bone marrow (B), spleen (S) and liver (Li). In some mice the persistence of giant platelets in the peripheral blood is seen as well (pl, top inset). All magnifications are 100 \times . See Figure 2A for normal controls. **(C)** Leukemic *NUP98-HOXA9* cells infiltrate multiple organs and are predominantly monoclonal. Top panel: Southern blot analysis for the integrity of the provirus. The *NUP98-HOXA9* provirus is present, and in most mice (except #17) intact, in the genomic DNA of the bone marrow (B), spleen (S), thymus (T), lymph nodes (N), liver (Li), lung (Lu) and kidney (K). Bottom panel: Southern blot analysis for the clonality of the leukemic samples shows that, for the majority, a single *NUP98-HOXA9*-containing clone is present. For mouse #8, multiple clones can be seen in the spleen, but only the leukemic clone infiltrates organs such as the kidneys (#8, K). B.2 refers to the bone marrow from secondary mouse #2, which received leukemic bone marrow cells from the primary mouse. Lane C, genomic DNA from the bone marrow of a control B6C3 mouse; lane NH, 20 pg of digested plasmid DNA of the *NUP98-HOXA9* virus. The time at which animals were analyzed (in days post-BMT) and the number of cells transplanted to secondary recipients are shown at the bottom.

Table III. Generation of *Meis1/NUP98–HOXA9* hemopoietic chimeras

ID: NM# ^a (5 mice per group)	Symbol ^b	No. of infected CFC transplanted per mouse ^c	
		<i>NUP98–HOXA9</i>	<i>Meis1 + NUP98–HOXA9</i>
1–5	cross	ND ^d	ND
6–10	cross	340	13
11–15	circle	13 900	1200
16–20	diamond	5700	1400

^aMice: NM# 1–5, *NUP98–HOXA9(Neo)* virus; NM# 6–20, *NUP98–HOXA9(EGFP)*; NM# 1–10, *Meis1(Pac)* virus; NM# 11–20, *Meis1(EYFP)* virus.

^bSymbols are used to represent mice from each group in Figure 4C.

^cNot shown are CFC infected with only the *Meis1* virus, as these cells are not leukemogenic.

^dNot determined.

The fusion protein has lost this portion of HOXA9 (altering the results of collaboration with *Meis1*), but has the capacity to induce MPD, which is not observed in *Hoxa9* mice (Kroon *et al.*, 1998) and may potentially be supplied by the NUP98 portion of the fusion protein.

***Hoxa9ΔN* does not induce a disease in mice**

To address these issues, a deletion mutant of *Hoxa9* corresponding to the portion present in the fusion protein was created. Although the murine *Hoxa9* was used, it is 99% identical to the human HOXA9 protein within the 107 C-terminal amino acids remaining in *Hoxa9ΔN*. Figure 5A shows a schematic representation of *Hoxa9ΔN*, and that efficient expression of the truncated protein was obtained in cells infected with the *Hoxa9ΔN* virus.

To assess the importance of the *NUP98* portion with respect to the induction of MPD and AML by *NUP98–HOXA9*, five *Hoxa9ΔN* chimeras were generated (transplantation dose: 1730 CFC per mouse, ~20% infected). These mice were shown to be reconstituted with transduced bone marrow cells, as determined by the presence of G-418 resistant CFC in the bone marrow and spleen (30–60% of total CFC), and by Southern blot analysis (Figure 5B). None of the mice showed any signs of hemopoietic anomalies for up to 16 months post-transplantation (spleen size normal, CFC numbers within normal range, data not shown). Similarly, *Meis1/Hoxa9ΔN* chimeras do not acquire any hemopoietic disease (data not shown). These results indicated that the N-terminal portion of *Hoxa9* plays an important role in leukemogenesis and collaboration with *Meis1*. Replacing it with a portion of *NUP98* results in a fusion protein with the capacity to induce MPD and partial collaboration with *Meis1* to induce AML.

Discussion

The t(7;11)(p15;p15) translocation that results in the expression of the *NUP98–HOXA9* fusion gene is predominantly observed in patients with AML M2 and occasionally M4 French-American-British sub-types (Borrow *et al.*, 1996; Nakamura *et al.*, 1996a), trilineage MDS (Inaba *et al.*, 1996; Hatano *et al.*, 1999) and chronic myelomonocytic leukemia (Hatano *et al.*, 1999; Wong *et al.*, 1999). The retrovirally directed expression of *NUP98–HOXA9* in murine bone marrow cells resulted in enhanced proliferation of myeloid progenitor cells *in vitro* and in their expansion *in vivo*, inducing an MPD in mice.

After a period of several months, during which the hemopoietic stem cell-derived MPD progressed, bone marrow cells expressing *NUP98–HOXA9* fully transformed to induce AML. The transformation from *NUP98–HOXA9*-induced MPD into AML is accelerated by the co-expression of *Meis1*. The *NUP98* moiety of the fusion protein appears to be critical in the development of the MPD, converting a clinically silent pre-leukemic phase observed in *Hoxa9* mice into an MPD in *NUP98–HOXA9* mice. Comparison of bone marrow cells expressing *Hoxa9* versus *NUP98–HOXA9* suggest that the proliferative effect on myeloid progenitors is greater for *NUP98–HOXA9*, while the capacity to induce AML is superior for *Hoxa9*, thus potentially indicating that proliferation and transformation proceed independently.

Molecular and cellular bases for NUP98–HOXA9-induced leukemic transformation

A trimeric, *Meis1*- and *Pbx2*-containing complex has been proposed as a model for leukemic transformation induced by *Hoxa9* (Schnabel *et al.*, 2000). Studies by Kasper *et al.* (1999) showed that *NUP98–HOXA9* can form a cooperative DNA-binding complex with *PBX1* and that this interaction is required for the transformation of fibroblasts. We have also reported that certain *Hox* genes collaborate with *Pbx1* in transforming Rat-1 fibroblast (Krosel *et al.*, 1998). In contrast to *Hox*-induced transformation of fibroblasts, several studies indicate that *Hox* proteins function in the absence of interaction with *PBX* to immortalize or transform primary hemopoietic cells. Key findings to support this include: (i) the *in vitro* immortalization of myeloid progenitor cells by tryptophan mutants of *Hoxa9* (i.e. in which interaction with *PBX* is abrogated) (Calvo *et al.*, 2000); (ii) the *in vivo* expansion of hemopoietic stem cells by a similarly mutated *Hoxb4* protein incapable of interaction with *PBX* (Beslu *et al.*, 2000); and, most relevant to this paper, (iii) the capacity of the *NUP98–HOXD13* fusion protein [the product of the t(2;11)(q31;p15) translocation, which occasionally occurs in human leukemias] to induce transformation of bone marrow cells (Raza-Egilmez *et al.*, 1998; Buske *et al.*, 2000). The HOX family members from paralogs 11–13, including HOXD13, lack a *PBX*-interaction motif N-terminal to the homeodomain, which is critical for cooperative DNA-binding with *PBX* proteins (Knoepfler *et al.*, 1995; Piper *et al.*, 1999). HOXD13 is, therefore, amongst the HOX proteins that fail to engage in cooperative DNA binding with *PBX* (Shen *et al.*, 1997).

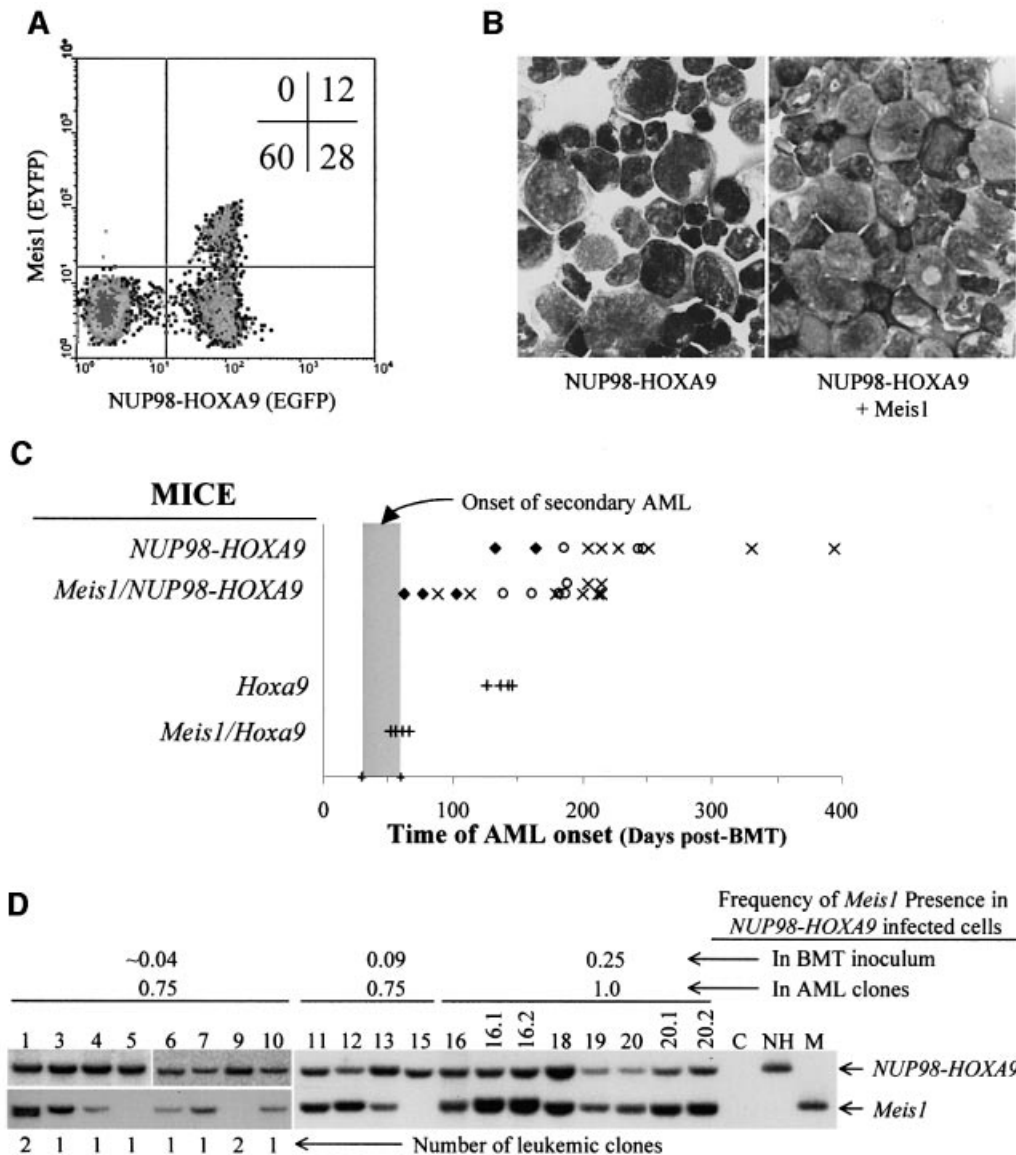


Fig. 4. *Meis1* accelerates the transformation of *NUP98-HOXA9*-induced MPD into AML. (A) The contribution of cells infected with *NUP98-HOXA9* (EGFP⁺) versus *Meis1* and *NUP98-HOXA9* (EYFP⁺/EGFP⁺) in mice with MPD is similar to the input BMT inoculum. Shown is a FACS profile of splenic cells from mouse NM# 16. In the BMT inoculum, 20% of *NUP98-HOXA9*-infected cells also contained the *Meis1* provirus (see Table III), while in the spleen of this mouse 30% of the EGFP⁺ cells are also EYFP⁺. The lack of single EYFP⁺ (*Meis1*-infected) cells indicates that only *NUP98-HOXA9*-expressing cells contribute to the MPD. (B) Comparison of immature myeloid cells in the bone marrow of leukemic *NUP98-HOXA9* versus *Meis1/NUP98-HOXA9* mice. (C) Time of onset of AML is shown for mice that were transplanted with bone marrow cells infected with *NUP98-HOXA9* (AML onset 230 ± 67 days post-BMT), *Meis1* plus *NUP98-HOXA9* (142 ± 52 days), *Hoxa9* (BMT dose, 700 transduced CFC per mouse, AML onset 128 ± 15 days) and *Meis1* plus *Hoxa9* (100 doubly transduced CFC per mouse, AML onset 57 ± 6 days). The three mice in the *Meis1/NUP98-HOXA9* group whose leukemic cells lacked the *Meis1* provirus (see D) are indicated by slightly raised symbols. Symbols refer to different groups of mice, see Tables I and III. Note that despite the low BMT doses, AML in *Meis1/Hoxa9* mice develop more rapidly than in *Meis1/NUP98-HOXA9* mice. (D) Southern blot analyses of genomic DNA from the bone marrow of leukemic *Meis1/NUP98-HOXA9* mice shows the presence of the *NUP98-HOXA9* provirus in all samples (lanes are numbered according to mouse numbers in Table III), while the *Meis1* provirus is detected in all mice except NM# 5, 9 and 15. DNA from secondary transplants were loaded in lanes 16.1, 16.2, 20.1 and 20.2. For mice NM# 1–10, the *NUP98-HOXA9* provirus was detected with the *Neo* (1–5) or the *EGFP* (6–10) probes, while the *Meis1* provirus was detected with the *Pac* probe. For mice NM# 11–20, the *EGFP* probe was used to detect both proviruses. Lane C, DNA from a B6C3 control mouse; 20 pg of digested plasmid DNA of the *NUP98-HOXA9* and *Meis1* viral vectors were loaded in lanes NH and M, respectively.

Together these findings suggest that transformation of primary bone marrow cells by *NUP98-HOXA9* may not be dependent on interaction with PBX. This issue was directly addressed by the generation of a mutant *NUP98-HOXA9* protein containing a tryptophan to glycine mutation previously shown to abrogate PBX interaction (Kasper *et al.*, 1999; Schnabel *et al.*, 2000).

This mutant was comparable to *NUP98-HOXA9* in its capacity to dramatically enhance the proliferative capacity of primary bone marrow progenitors (E.Kroon, unpublished observations). Together these data strongly suggest that cooperative DNA binding between *NUP98-HOXA9* and PBX proteins does not represent the biochemical basis for transformation of primary bone marrow cells.

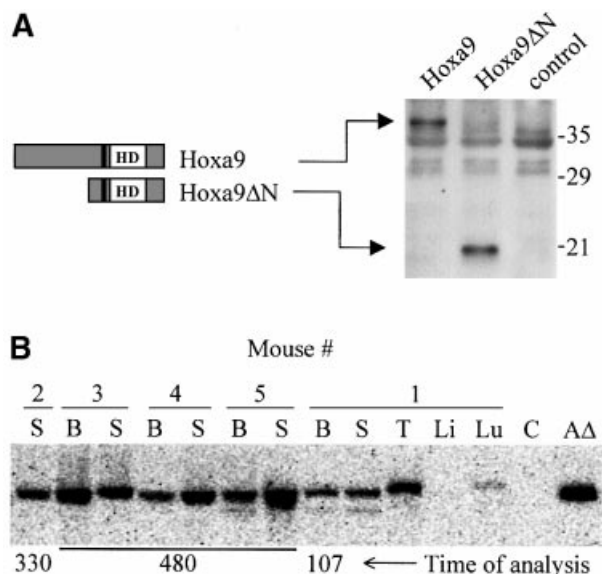


Fig. 5. *Hoxa9ΔN* chimeras are reconstituted with transduced cells. Schematic representations of Hoxa9 and Hoxa9ΔN and the demonstration that the recombinant retroviruses direct the expression of the appropriate proteins in infected cells (A), and that *Hoxa9ΔN* chimeras are reconstituted by cells containing the *Hoxa9ΔN* provirus (B). (A) Western blot analysis of total cell extracts of Hoxa9-, Hoxa9ΔN-expressing and control GP+E-86 viral producer cells, probed with antiserum raised against a NUP98–HOXA9 peptide (see Figure 1A). HD, DNA-binding homeodomain; the tryptophan required for Hoxa9 interaction with its PBX DNA-binding partners (Schnabel *et al.*, 2000) is represented by the black line N-terminal to the HD, and is retained in Hoxa9ΔN, which consists of the C-terminal 107 amino acids of Hoxa9. (B) Southern blot analysis shows the presence of the *Hoxa9ΔN* provirus in hemopoietic organs (bone marrow, B; spleen, S; thymus, T; liver, Li; lung, Lu). Lane C, DNA from B6C3 mouse; lane AA, 20 pg of digested plasmid DNA of the *Hoxa9ΔN* viral vector.

The apparent lack of biochemical interaction between NUP98–HOXA9 and PBX proteins in the transformation of hemopoietic cells does not rule out a role for PBX, specifically in the collaboration between Meis1 and NUP98–HOXA9. Members of the Meis family, including Meis1 (Rieckhof *et al.*, 1997) and Prep1 (Berthelsen *et al.*, 1999), can regulate the nuclear localization of PBX proteins. However, this activity does not appear to be sufficient for collaboration with HOX proteins in leukemogenesis, since we failed to see a genetic interaction between *Hoxa9* and *Prep1* (Thorsteinsdottir *et al.*, 2001), or between *NUP98–HOXA9* and *Prep1* (E.Kroon, unpublished observations) in hemopoietic chimeras.

Unlike *Hoxa9*, NUP98–HOXA9 appears to have a strong transcriptional activating potential mediated through the interaction with CBP/p300 (Kasper *et al.*, 1999). Both CBP and p300 have been implicated in leukemogenesis as MLL fusion proteins (Ida *et al.*, 1997; Rowley *et al.*, 1997; Taki *et al.*, 1997) and through direct interaction with AML1 (Kitabayashi *et al.*, 1998). Despite this, our results suggest that the potential of *Hoxa9* to induce AML is superior to that of NUP98–HOXA9 (in the presence or absence of *Meis1* expression, Figure 4C). More recently, a transcriptionally active domain in the N-terminal portion of *Hoxa9* (deleted in NUP98–HOXA9) was identified and appears necessary for *in vitro* immortalization of hemopoietic cells (Schnabel *et al.*, 2000).

Thus, distinct transcriptionally active domains in *Hoxa9* and NUP98–HOXA9 are required for their transforming potential *in vitro*, and this may contribute to the different phenotypes observed in *Hoxa9* versus NUP98–HOXA9 chimeric mice.

Important differences were observed between *Hoxa9* and NUP98–HOXA9 hemopoietic chimeras in both the pre-leukemic phenotype (i.e. chronic disease for NUP98–HOXA9, none observed for *Hoxa9*) and in the time required for the onset of the primary AML (faster for *Hoxa9* in the presence or absence of *Meis1* expression, see Figure 4C). These differences may also suggest that distinct cell types participated in the leukemic process induced by these two molecules. It could be argued that NUP98–HOXA9 has a more profound effect on mature progenitors (detected by *in vitro* assays), while *Hoxa9* affects more primitive bone marrow cells (U.Thorsteinsdottir, unpublished data). Regardless of the underlying molecular reasons for different cell types being affected, it is tempting to speculate that this could in part be responsible for the differences observed in the latency prior to AML onset. In other words, the number of additional transforming events required to achieve acute leukemia (or the probability that such events take place) may depend on the target cell. Alternatively, *Hoxa9* may have a larger repertoire of potential collaborating events than NUP98–HOXA9, a possibility we are currently investigating.

In summary, the studies detailed here document common as well as distinct characteristics of a chimeric (NUP98–HOXA9) and a native (*Hoxa9*) protein when expressed in bone marrow cells of mice. While the fusion protein is less potent in acute leukemogenesis and has the unique capacity to induce a chronic disease, both share a common leukemogenic collaborator, Meis1.

Materials and methods

Animals

Bone marrow donor PepC3 (C57BL/6Ly-Pep3b × C3H/HeJ, F1) and recipient B6C3 (C57BL/6J × C3H/HeJ, F1) mice were housed in ventilated micro-isolator cages and provided with sterilized food and acidified water.

Recombinant retroviral vectors

The cDNA of NUP98–HOXA9 (Nakamura *et al.*, 1996a) was introduced into the *EcoRI* site of retroviral vectors MSCV/pgk/NeoEB (No. 619) (Hawley *et al.*, 1994) or MSCV/pgk/EGFP (No. 662) (a gift from K.Humphries, Terry Fox Laboratory, Vancouver, BC, Canada). The recombinant retroviruses directing the expression of *Hoxa9* (No. 412) and *Meis1a* (No. 515) were previously described (Kroon *et al.*, 1998). The MSCV/pgk/EYFP vector (No. 721) was constructed by replacing the *NcoI–ClaI* fragment of MSCV/pgk/EGFP (No. 652) with the *NcoI–ClaI* EYFP cDNA fragment obtained from pN1-EYFP (Clontech). MSCV/Meis1a/pgk/EYFP (No. 722) was created by introducing the *Meis1a* (Moskow *et al.*, 1995) cDNA fragment into the *EcoRI* site of MSCV/pgk/EYFP. *Hoxa9ΔN* was generated by PCR, sequenced and introduced into the *HpaI* site of MSCV/pgk/NeoEB (No. 464). The W→G mutation of *Hoxa9* was PCR generated and sequenced, and the fragment downstream of the *ClaI* site was used to replace the corresponding region of NUP98–HOXA9 to create NUP98–HOXA9(W→G) in MSCV/pgk/EGFP (No. 1090) and MSCV/pgk/EYFP (No. 1087).

Viral producer cell lines and infection of bone marrow cells

High-titer, helper-free GP+E-86 (Markowitz *et al.*, 1988) producer cells were generated by infection with viral supernatant obtained from VSV-G cells (Ory *et al.*, 1996) and maintained as described (Sauvageau *et al.*, 1995; Kroon *et al.*, 1998). Bone marrow cells were harvested, pre-

stimulated, infected through co-cultivation with GP+E-86 cells, recovered, and injected intravenously into lethally irradiated recipients as described (Sauvageau *et al.*, 1995; Kroon *et al.*, 1998). Gene transfer efficiencies were determined by flow cytometry and/or clonogenic progenitor assays (Sauvageau *et al.*, 1995; Kroon *et al.*, 1998).

In vitro clonogenic progenitor assays

For myeloid clonogenic progenitor assays, cells were plated in 35 mm petri dishes in a 1.1 ml culture mixture containing 1% methylcellulose in alpha medium supplemented with 10% fetal calf serum (FCS), 5.7% bovine serum albumin (BSA), 5×10^{-5} M β -mercaptoethanol, 1 U/ml human urinary erythropoietin (Epo), 10% WEHI-3B-conditioned medium, 2 mM glutamine, 200 μ g/ml transferrin, in the presence or absence of 1.3 mg/ml G418 and/or 1.3 μ g/ml puromycin. Bone marrow cells harvested from the co-cultivation with viral producer cells were plated at a concentration of $1-5 \times 10^3$ cells/ml, while bone marrow or spleen cells recovered from reconstituted animals were plated at $2-5 \times 10^4$ cells/ml and $2-100 \times 10^4$ cells/ml, respectively, and scored on day 12. For pre-B-lymphoid clonogenic progenitor assays, 10^5 bone marrow cells were plated in 1% methylcellulose in alpha medium supplemented with 30% FCS, 10^{-4} M β -mercaptoethanol, 2 mM glutamine, 0.2 ng/ml IL-7, in the presence or absence of 1.3 mg/ml G418, and scored on day 8.

DNA and RNA analyses

Southern blot analyses were performed as described previously (Sauvageau *et al.*, 1995; Kroon *et al.*, 1998). Briefly, to assess the integrity of the provirus, high-molecular weight genomic DNA was prepared with the DNAzol reagent (Gibco-BRL) and 10 μ g digested with *KpnI* or *NheI*, which cleave in the LTRs, thus releasing identical fragments for all proviruses unless rearrangement occurred. The expression of the integrated provirus was always confirmed through northern blot analysis (Sauvageau *et al.*, 1995; Kroon *et al.*, 1998). To survey for proviral integration sites (revealing the clonality of the sample), the DNA was digested with *EcoRI*, which cleaves within the provirus to release a unique DNA fragment for each proviral integration site. 32 P probes of *EGFP* (*NcoI*-*Clai* fragment of MSCV/pgk1/*EGFP*), *Neo* (Sauvageau *et al.*, 1995; Kroon *et al.*, 1998), *Pac* (Sauvageau *et al.*, 1995; Kroon *et al.*, 1998) and *NUP98-HOXA9* (3' *HindIII* fragment, see Figure 1) were generated using standard techniques.

Flow cytometry

For FACS analyses, cells from the peripheral blood, bone marrow, spleen and thymus were incubated with phycoerythrin-(PE) or biotin-conjugated monoclonal antibodies. The following antibodies were used: anti-Mac-1 (CD11b)-biotin, anti-B220 (CD45R)-PE, anti-CD4-biotin (all from Pharmingen, San Diego, CA) and anti-CD-8-PE (Gibco-BRL Life Technologies).

Protein analysis

Preparation of cellular extracts of transduced Rat-1 fibroblasts or GP+E-86 cells and western analysis were performed as described (Kroon *et al.*, 1998). Briefly, 30 μ g of proteins were separated by 10% SDS-PAGE, transferred to Immobilon P membranes (Millipore, Bedford, MA), and then probed with polyclonal rabbit NUP98-HOXA9 antiserum (see Figure 1). Bound antibodies were detected with horseradish peroxidase-conjugated anti-rabbit antibody (Sigma, St Louis, MO) followed by enhanced chemiluminescence (ECL; Amersham, Buckinghamshire, UK).

Acknowledgements

This work was supported by grants from the National Cancer Institute of Canada and the US National Institute of Health. The authors acknowledge Drs Alex Hendrick and Angela Wood for advice and critical review of this manuscript; Mrs Marie-Eve Leroux and Mr Stephan Matte for their expertise and help regarding maintenance and manipulation of mice; Mrs Nathalie Tessier for her assistance with flow cytometry; and Mr Soheyl Baban for the generation of *Hoxa9 Δ N*. E.K. and U.T. are Fellows of the Leukemia & Lymphoma Society of America and the Leukemia Research Fund of Canada, respectively, and G.S. is a Clinician-Scientist Scholar of the Medical Research Council of Canada.

References

Arai, Y., Hosoda, F., Kobayashi, H., Arai, K., Hayashi, Y., Kamada, N., Kaneko, Y. and Ohki, M. (1997) The inv(11)(p15q22) chromosome

translocation of *de novo* and therapy-related myeloid malignancies results in fusion of the nucleoporin gene, NUP98, with the putative RNA helicase gene, DDX10. *Blood*, **89**, 3936-3944.

Berthelsen, J., Kilstrup-Nielsen, C., Blasi, F., Mavilio, F. and Zappavigna, V. (1999) The subcellular localization of PBX1 and EXD proteins depends on nuclear import and export signals and is modulated by association with PREP1 and HTH. *Genes Dev.*, **13**, 946-953.

Beslu, N., Kros, J., Girard, S., Mayotte, N., Antonchuk, J., Humphries, K. and Sauvageau, G. (2000) The N-terminal amino acids 31-100 and the homeodomain delineate regions of HOXB4 involved in hemopoietic stem cell expansion. *Blood*, **96**, 496.

Borrow, J. *et al.* (1996) The t(7;11)(p15;p15) translocation in acute myeloid leukaemia fuses the genes for nucleoporin NUP98 and class I homeoprotein HOXA9. *Nature Genet.*, **12**, 159-167.

Buske, C., Pineault, N., Feuring-Buske, M., Aplan, P. and Humphries, R.K. (2000) Collaboration of Meis1 with the human leukemia-specific fusion gene NUP98-HOXA13 causes Acute Myeloid Leukemia (AML) in mice: a model of NUP98-associated human leukemia. *Blood*, **96**, 573.

Calvo, K.R., Sykes, D.B., Pasillas, M. and Kamps, M.P. (2000) Hoxa9 immortalizes a granulocyte-macrophage colony-stimulating factor-dependent promyelocyte capable of biphenotypic differentiation to neutrophils or macrophages, independent of enforced Meis expression. *Mol. Cell. Biol.*, **20**, 3274-3285.

Chang, C.P., Shen, W.F., Rozenfeld, S., Lawrence, H.J., Largman, C. and Cleary, M.L. (1995) Pbx proteins display hexapeptide-dependent cooperative DNA binding with a subset of Hox proteins. *Genes Dev.*, **9**, 663-674.

Chang, C.P., Jacobs, Y., Nakamura, T., Jenkins, N.A., Copeland, N.G. and Cleary, M.L. (1997) Meis proteins are major *in vivo* DNA binding partners for wild-type but not chimeric Pbx proteins. *Mol. Cell. Biol.*, **17**, 5679-5687.

Golub, T.R. *et al.* (1999) Molecular classification of cancer: class discovery and class prediction by gene expression monitoring. *Science*, **286**, 531-537.

Hatano, Y., Miura, I., Nakamura, T., Yamazaki, Y., Takahashi, N. and Miura, A.B. (1999) Molecular heterogeneity of the NUP98/HOXA9 fusion transcript in myelodysplastic syndromes associated with t(7;11)(p15;p15). *Br. J. Haematol.*, **107**, 600-604.

Hawley, R.G., Fong, A., Lu, M. and Hawley, T.S. (1994) The HOX11 homeobox-containing gene of human leukemia immortalizes murine hematopoietic precursors. *Oncogene*, **9**, 1-12.

Ida, K., Kitabayashi, I., Taki, T., Taniwaki, M., Noro, K., Yamamoto, M., Ohki, M. and Hayashi, Y. (1997) Adenoviral E1A-associated protein p300 is involved in acute myeloid leukemia with t(11;22)(q23;q13). *Blood*, **90**, 4699-4704.

Ikeda, T., Ikeda, K., Sasaki, K., Kawakami, K. and Takahara, J. (1999) The inv(11)(p15q22) chromosome translocation of therapy-related myelodysplasia with NUP98-DDX10 and DDX10-NUP98 fusion transcripts. *Int. J. Hematol.*, **69**, 160-164.

Inaba, T. *et al.* (1996) t(7;11) and trilineage myelodysplasia in acute myelomonocytic leukemia. *Cancer Genet. Cytogenet.*, **86**, 72-75.

Kasper, L.H., Brindle, P.K., Schnabel, C.A., Pritchard, C.E., Cleary, M.L. and van Deursen, J.M. (1999) CREB binding protein interacts with nucleoporin-specific FG repeats that activate transcription and mediate NUP98-HOXA9 oncogenicity. *Mol. Cell. Biol.*, **19**, 764-776.

Kitabayashi, I., Yokoyama, A., Shimizu, K. and Ohki, M. (1998) Interaction and functional cooperation of the leukemia-associated factors AML1 and p300 in myeloid cell differentiation. *EMBO J.*, **17**, 2994-3004.

Knoepfler, P.S. and Kamps, M.P. (1995) The pentapeptide motif of Hox proteins is required for cooperative DNA binding with Pbx1, physically contacts Pbx1, and enhances DNA binding by Pbx1. *Mol. Cell. Biol.*, **15**, 5811-5819.

Kroon, E., Kros, J., Thorsteinsdottir, U., Baban, S., Buchberg, A.M. and Sauvageau, G. (1998) Hoxa9 transforms primary bone marrow cells through specific collaboration with Meis1a but not Pbx1b. *EMBO J.*, **17**, 3714-3725.

Kros, J., Baban, S., Kros, G., Rozenfeld, S., Largman, C. and Sauvageau, G. (1998) Cellular proliferation and transformation induced by HOXB4 and HOXB3 proteins involves cooperation with PBX1. *Oncogene*, **16**, 3403-3412.

Markowitz, D., Goff, S. and Bank, A. (1988) A safe packaging line for gene transfer: separating viral genes on two different plasmids. *J. Virol.*, **62**, 1120-1124.

Moskow, J.J., Bullrich, F., Huebner, K., Daar, I.O. and Buchberg, A.M.

- (1995) Meis1, a PBX1-related homeobox gene involved in myeloid leukemia in BXH-2 mice. *Mol. Cell. Biol.*, **15**, 5434–5443.
- Nakamura, T. *et al.* (1996a) Fusion of the nucleoporin gene NUP98 to HOXA9 by the chromosome translocation t(7;11)(p15;p15) in human myeloid leukaemia. *Nature Genet.*, **12**, 154–158.
- Nakamura, T., Largaespada, D.A., Shaughnessy, J.D., Jenkins, N.A. and Copeland, N.G. (1996b) Cooperative activation of Hoxa and Pbx1-related genes in murine myeloid leukaemias. *Nature Genet.*, **12**, 149–153.
- Nakamura, T., Yamazaki, Y., Hatano, Y. and Miura, I. (1999) NUP98 is fused to PMX1 homeobox gene in human acute myelogenous leukemia with chromosome translocation t(1;11)(q23;p15). *Blood*, **94**, 741–747.
- Nishiyama, M. *et al.* (1999) 11p15 translocations involving the NUP98 gene in childhood therapy-related acute myeloid leukemia/myelodysplastic syndrome. *Genes Chromosomes Cancer*, **26**, 215–220.
- Ory, D., Neugeborne, B.A. and Mulligan, R.C. (1996) A stable human-derived packaging cell line for production of high titer retrovirus/vesicular stomatitis virus G pseudotypes. *Proc. Natl Acad. Sci. USA*, **93**, 11400–11406.
- Phelan, M.L., Rambaldi, I. and Featherstone, M.S. (1995) Cooperative interaction between HOX and PBX proteins mediated by a conserved peptide motif. *Mol. Cell. Biol.*, **15**, 3989–3997.
- Piper, D.E., Batchelor, A.H., Chang, C.P., Cleary, M.L. and Wolberger, C. (1999) Structure of a HoxB1–Pbx1 heterodimer bound to DNA: role of the hexapeptide and a fourth homeodomain helix in complex formation. *Cell*, **96**, 587–597.
- Raza-Egilmez, S.Z., Jani-Sait, S.N., Grossi, M., Higgins, M.J., Shows, T.B. and Aplan, P.D. (1998) NUP98–HOXD13 gene fusion in therapy-related acute myelogenous leukemia. *Cancer Res.*, **58**, 4269–4273.
- Rieckhof, G.E., Casares, F., Don Ryoo, H., Abu-Shaar, M. and Mann, R.S. (1997) Nuclear translocation of extradenticle requires *homothorax*, which encodes an extradenticle-related homeodomain protein. *Cell*, **91**, 171–183.
- Rowley, J.D. *et al.* (1997) All patients with the t(11;16)(q23;p13.3) that involves MLL and CBP have treatment-related hematologic disorders. *Blood*, **90**, 535–541.
- Sauvageau, G., Thorsteinsdottir, U., Eaves, C.J., Lawrence, H.J., Largman, C., Lansdorp, P.M. and Humphries, R.K. (1995) Over-expression of HOXB4 in hematopoietic cells causes the selective expansion of more primitive populations *in vitro* and *in vivo*. *Genes Dev.*, **9**, 1753–1765.
- Schnabel, C.A., Jacobs, Y. and Cleary, M.L. (2000) HoxA9-mediated immortalization of myeloid progenitors requires functional interactions with TALE cofactors Pbx and Meis. *Oncogene*, **19**, 608–616.
- Shen, W.F., Rozenfeld, S., Lawrence, H.J. and Largman, C. (1997) The Abd-B-like Hox homeodomain proteins can be subdivided by the ability to form complexes with Pbx1a on a novel DNA target. *J. Biol. Chem.*, **272**, 8198–8206.
- Shen, W.F., Rozenfeld, S., Kwong, A., Kom ves, L.G., Lawrence, H.J. and Largman, C. (1999) HOXA9 forms triple complexes with PBX2 and MEIS1 in myeloid cells. *Mol. Cell. Biol.*, **19**, 3051–3061.
- Taki, T., Sako, M., Tsuchida, M. and Hayashi, Y. (1997) The t(11;16)(q23;p13) translocation in myelodysplastic syndrome fuses the MLL gene to the CBP gene. *Blood*, **89**, 3945–3950.
- Thorsteinsdottir, U., Sauvageau, G. and Humphries, R.K. (1999) Enhanced *in vivo* regenerative potential of HOXB4-transduced hematopoietic stem cells with regulation of their pool size. *Blood*, **94**, 2605–2612.
- Thorsteinsdottir, U., Kroon, E., Jerome, L., Blasi, F. and Sauvageau, G. (2001) Defining Roles for *HOX* and *Meis1* genes in the induction of Acute Myeloid Leukemia. *Mol. Cell. Biol.*, **21**, 224–234.
- Wong, K.F., So, C.C. and Kwong, Y.L. (1999) Chronic myelomonocytic leukemia with t(7;11)(p15;p15) and NUP98/HOXA9 fusion. *Cancer Genet. Cytogenet.*, **115**, 70–72.

Received July 20, 2000; revised and accepted December 11, 2000